

Theoretical study of laser intensity noise effect on CW-STED microscopy

ALEJANDRO MENDOZA-COTO¹, DANAY MANZO JAIME², ARIEL FRANCIS PÉREZ MELLOR³, AND IVÁN COTO HERNÁNDEZ^{4,*}

¹Departamento de Física, Universidade Federal de Santa Catarina, 88040-900 Florianópolis, Santa Catarina, Brazil

²Department of Mechanical Engineering, Universidade Federal de Santa Catarina, Florianópolis, Brazil

³Department of Physical Chemistry, University of Geneva, Switzerland

⁴Surgical Photonics and Engineering Laboratory, Mass Eye and Ear and Harvard Medical School, 243 Charles St., Boston, MA, USA 02114

*Corresponding author: ivancotohernandez@meei.harvard.edu

Compiled March 8, 2022

Spatial resolution of stimulated emission depletion (STED) microscopy varies with sample labeling techniques and microscope components, e.g., lasers, lenses, and photo-detectors. Fluctuations in the intensity of the depletion laser decrease achievable resolution in STED microscopy; the stronger the fluctuations, the higher the average intensity needed to achieve a given resolution. This phenomenon is encountered in every STED measurement. However, a theoretical framework that evaluates the effect of intensity fluctuations on spatial resolution is lacking. This article presents an analytical formulation based on a stochastic model that characterizes the impact of the laser fluctuations and correlation time on the depletion efficiency in the continuous wave (CW) STED microscopy. We compared analytical results with simulations using a wide range of intensity noise conditions and found a high degree of agreement. The stochastic model used considers a colored noise distribution for the laser intensity fluctuations. Simple analytical expressions were obtained in the limit of small and large fluctuations correlation time. These expressions fitted very well the available experimental data. Finally, this work offers a starting point to model other laser noise effects in various microscopy implementations. © 2022 Optical Society of America

OCIS codes: (140.3460) Lasers; (180.2520) Fluorescence microscopy.

<http://dx.doi.org/10.1364/ao.XX.XXXXXX>

Stimulated emission depletion (STED) microscopy [1, 2] is a revolutionary imaging technique that provides a means of bypassing the diffraction limit of light, allowing biological samples to be observed in great detail. [3]. Its use has been widely explored, giving rise to multiple implementations and a growing number of biomedical publications. To improve the optical resolution of confocal microscopy, STED employs a second laser to deplete the fluorescence in the outer region of the diffraction-limited spot produced by the excitation laser.

A streamlined version of STED microscopy can be implemented with continuous-wave (CW) lasers, reducing tedious laser pulse preparation [4]. In addition, the progress of laser technology in the last two decades has allowed the implementation of CW-STED microscopy with inexpensive and compact lasers, such as visible-fiber lasers [5, 6], diode-pumped-solid-state lasers (DPSSLs) [7] and optical pumped-semiconductor lasers (OPSLs) [3].

Quantum and technical noises from laser sources generate intensity fluctuations [8] that can affect image contrast. Outstanding results in STED microscopy have been obtained with low-noise DPSS and OPSL lasers [3, 5]: which have a root mean square noise less than 0.1 %. Coto Hernández, I. et al. [9] have experimentally shown that the use of a low-noise STED laser reduces the intensity needed to achieve super-resolution. Laser noise can be characterized by its frequency-dependent power spectral density, often measured with a photodiode and electronic spectrum analyzer [9]. Furthermore, it can be analyzed through its intensity fluctuation or correlation time. White noise, uncorrelated noise, is a stochastic signal with constant power spectral density over the entire frequency range. In contrast, colored noise has a non-trivial power spectral distribution, often with a maximum or minimum at certain frequency value.

The performance of a super-resolution microscope can be characterized by spatial resolution. In practice, the achievable resolution depends not only on the optical properties of the system but also on the properties of the fluorophores such as photoswitching and labeling densities [10]. A straightforward approach to assess the performance or resolution of a STED microscope is to measure the depletion curve, which is defined as the normalized probability that an excited fluorophore contributes to the measured signal as a function of the STED beam intensity [11]. So far, STED microscopy theory considers the properties of the fluorophore and its transition under beam illumination to be noise-free. In addition, the potential bias in inhibition of fluorescence by stimulated emission due to fluctuations in the intensity of the STED beam are neglected. To overcome this limitation, we present in this Letter an analytical formulation to measure the depletion function based on colored noise and continuous-wave (CW) depletion beam.

A. Theory

In what follows, we perform the calculation of the depletion, considering that the STED laser has a noisy component. We used a two-step fluorescence mechanism that only takes into account the ground electronic state S_0 and the first electronic excited state S_1 of the system (see Fig. 1).

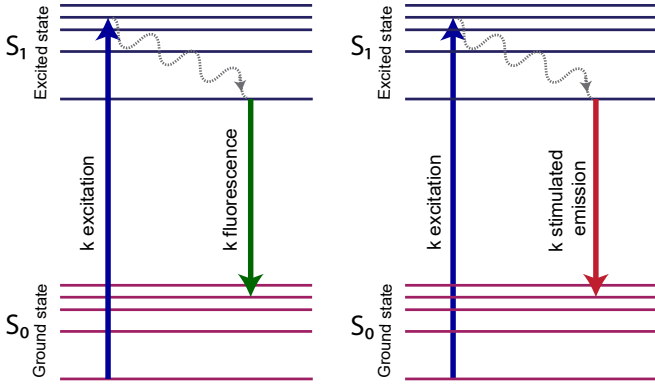


Fig. 1. Simplified Jablonski energy diagrams showing the processes of excitation, fluorescence and stimulated emission. The fluorophores are excited by an excitation laser. Then, the excited molecules relax to the ground state via spontaneous or stimulated emission induced by a second laser.

The fluorescence signal is proportional to $N_1(t)$, which is obtained by solving the following set of stochastic differential equations (SDE) where $N_0(t)$ and $N_1(t)$ are the corresponding ground and excited-state normalized populations, respectively.

$$\begin{aligned} \frac{dN_0(t)}{dt} &= -k_e \cdot N_0(t) + k_s(t) \cdot N_1(t) + k_f \cdot N_1(t) \\ \frac{dN_1(t)}{dt} &= -k_f \cdot N_1(t) - k_s(t) \cdot N_1(t) + k_e \cdot N_0(t) \end{aligned} \quad (1)$$

The parameter k_e represents the excitation rate from S_0 to S_1 while k_f represents the probability of emitting a photon in the relaxation process from S_1 . For simplicity, these two quantities are assumed to be independent of time. The time-dependent $k_s(t)$ function considers the rate of stimulated emission induced by the depletion laser. Given the linear relationship between $k_s(t)$ and the intensity of the depletion laser, $I_s(t)$ ($k_s(t) = \sigma_s I_s(t)$), they will share the same stochastic properties. The proportionality constant σ_s is the cross-section of the stimulated emission. The intensity of the STED laser can be seen as the fluctuation function $\delta I_s(t)$ relative to the average laser intensity $\langle I_s \rangle$, which is time-independent. Note that the latter is also valid for $k_s(t)$ such that, $k_s(t) = \langle k_s \rangle + \delta k_s(t)$. This, together with the fact that the sum of the populations of S_0 and S_1 is normalized ($N_0(t) + N_1(t) = 1$), allows for the simplification of the SDE as:

$$\frac{dN_1(t)}{dt} = -[k_f + \langle k_s \rangle + k_e] \cdot N_1(t) + k_e - \delta k_s(t) \cdot N_1(t) \quad (2)$$

This equation is a multiplicative noise stochastic differential equation [12, 13], and its solution is the cornerstone of this study. There are mainly two different ways to proceed based on the interpretations of Ito and Stratonovich. The two are entirely equivalent, the main difference being that the Stratonovich integrals are defined so that the chain rule of ordinary calculus

holds. Therefore, we use the Stratonovich interpretation in what follows.

The Eq. (2) can be rewritten as,

$$\frac{dN_1(\bar{t})}{d\bar{t}} = - \left[1 + \frac{\delta k_s(\bar{t})}{K} \right] N_1(\bar{t}) + \frac{k_e}{K} \quad (3)$$

where $\bar{t} = K \cdot t$ is a dimensionless variable and $K = k_f + \langle k_s \rangle + k_e$ represents the sum of all the time-independent rates. From here on, we will omit the tilde mark over "t" to avoid cumbersome notation.

To proceed, we need to specify the nature of the noise δk_s , and in our case, we will consider the well known colored Ornstein-Uhlenbeck noise. This choice enables us to simultaneously study the effects of noise variance and correlation time on the depletion value. The noise δk_s can be generated through the Ornstein-Uhlenbeck equation

$$\frac{d}{dt} \delta k_s(t) = -\lambda \cdot \delta k_s(t) + \lambda \cdot \beta(t) \quad (4)$$

where $\beta(t)$ is a white noise of auto-correlation function $\langle \beta(t) \beta(t') \rangle = \Delta \cdot \delta(t - t')$ and Δ its variance. The parameter $\lambda = \tau^{-1}$ represents the inverse of the characteristic correlation time. In addition, we simply consider $\delta k_s(0) = 0$ as the initial condition. This particular model proposed for $\delta k_s(t)$ guarantees that in the limit $t \rightarrow \infty$ and $\lambda \rightarrow \infty$ (Gaussian white noise limits), $\langle \delta k_s(t) \delta k_s(t') \rangle = \Delta \cdot \delta(t - t')$. It means that by varying the characteristic correlation time in Eq.4 we can interpolate between the Gaussian white noise limit and a highly time-correlated Ornstein-Uhlenbeck noise. For the last process, a direct calculation [14] allows us to obtain the auto-correlation function such as:

$$\begin{aligned} \langle \delta k_s(t) \cdot \delta k_s(t') \rangle &= \frac{\Delta \cdot \lambda}{2} \exp[-\lambda \cdot |t - t'|] \\ &\quad - \frac{\Delta \cdot \lambda}{2} \exp[-\lambda \cdot (t + t')] \end{aligned} \quad (5)$$

which in the long time limit ($t, t' \gg \lambda^{-1}$) behave as:

$$\langle \delta k_s(t) \cdot \delta k_s(t') \rangle = \frac{\Delta \lambda}{2} \cdot \exp[-\lambda \cdot |t - t'|]. \quad (6)$$

The knowledge of the statistical properties of $\delta k_s(t)$ are crucial for the determination of the average population of our model $\langle N_1(t) \rangle$. This quantity will be used to calculate the depletion, which is defined as:

$$\eta = \frac{\langle N_1(+\infty, \langle k_s \rangle) \rangle}{\langle N_1(+\infty, 0) \rangle}. \quad (7)$$

where $\langle N_1(+\infty, \langle k_s \rangle) \rangle$ corresponds to the average population at $t \rightarrow \infty$, after taking the statistical average over realisations of $\delta k_s(t)$ and the normalization factor $\langle N_1(+\infty, 0) \rangle$ corresponds to the equilibrium population setting $k_s = 0$. The long time limit $t \rightarrow \infty$ is considered because, experimentally, the depletion is calculated assuming a steady-state condition. Physically η give the probability to force fluorophores to their ground off-state for a given STED laser power.

To calculate the average value of $\langle N_1(t) \rangle$, we proceed first with the solution of Eq. (3), using standard methods for solving linear differential equations [15]. In a second step, we take the statistical average of the solution, which yields

$$\begin{aligned} \langle N_1(t) \rangle &= N_1(0) \cdot \exp(-t) I(t, 0) \\ &\quad + \frac{k_e}{K} \int_0^t dt' \exp[-(t - t')] I(t, t'), \end{aligned} \quad (8)$$

where $N_1(0)$ is the initial population and the function $I(t, t')$ is given by the general expression

$$I(t, t') = \left\langle \exp \left[- \int_{t'}^t \frac{\delta k_s(t_2)}{K} dt_2 \right] \right\rangle \quad (9)$$

To continue with the determination of $I(t, t')$, we can now expand the exponential into its power series and then compute the corresponding average to the 2n-point correlation functions of $\delta k_s(t)$, evaluated at different times. Since we assume that $\delta k_s(t)$ is a Gaussian random variable we can always write the 2n-point correlation functions in terms of the two point correlation function $\langle \delta k_s(t_1) \delta k_s(t_2) \rangle$. The result obtained then allows a resummation of the series [16] after the formal integration over the time variables yielding

$$I(t, t') = \exp \left[\frac{1}{2K^2} \int_{t'}^t \int_{t'}^t \langle \delta k_s(t_1) \delta k_s(t_2) \rangle dt_1 dt_2 \right]. \quad (10)$$

If we now take into account the specific form of $\langle \delta k_s(t) \delta k_s(t') \rangle$ given in Eq. (5), we can calculate exactly the form of $I(t, t')$ and consequently the value of $\langle N_1(t) \rangle$ in the long time limit ($t \rightarrow \infty$). In this limit, we can verify that the contribution from the initial conditions from both $N_1(0)$ and $\delta k_s(0)$ are negligible for weak enough noise intensities ($\Delta < 2K^2$). The described procedure lead us to

$$\begin{aligned} \langle N_1(+\infty) \rangle &= \frac{k_e}{K} \cdot \exp \left(- \frac{\Delta}{2\lambda K^2} \right) \int_0^\infty \exp \left[- \left(u - \frac{\Delta}{2K^2} u \right) \right] \\ &\cdot \exp \left(\frac{\Delta}{2K^2 \lambda} e^{-\lambda u} \right) du. \end{aligned} \quad (11)$$

The integral above can be written in terms of Gamma and incomplete Gamma functions in the form:

$$\begin{aligned} \langle N_1(+\infty) \rangle &= \frac{k_e}{K} \cdot \exp \left(- \frac{\Delta}{2\lambda K^2} \right) \cdot \left(- \frac{\Delta}{2\lambda K^2} \right)^{-1 + \frac{\Delta}{2K^2}} \frac{1}{\lambda} \\ &\frac{1}{\lambda} \left[\Gamma \left(\frac{1 - \frac{\Delta}{2K^2}}{\lambda} \right) - \Gamma \left(\frac{1 - \frac{\Delta}{2K^2}}{\lambda}, - \frac{\Delta}{2K^2 \lambda} \right) \right]. \end{aligned} \quad (12)$$

Although this expression is not easy to interpret physically, it allows a straightforward calculation of the depletion, as defined in Eq. (7). Additionally, we can analyse the limit cases corresponding to $\lambda \rightarrow 0$ or $\Delta \rightarrow 0$ and $\lambda \rightarrow \infty$. The first scenario corresponds to the ideal case in which noise does not play any role and the second case when the colored noise becomes a white noise due to a reduction of the correlation time. For those cases, simple analytical expressions for depletion can be obtained allowing a direct physical interpretation of the results.

A.1. Ideal case, $\lambda \rightarrow 0$ or $\Delta \rightarrow 0$

In this limit, we recover $\langle N_1(+\infty) \rangle = k_e/K$, which lead us to

$$\eta = \left[1 + \frac{\langle k_s \rangle}{k_f + k_e} \right]^{-1}. \quad (13)$$

This result can be expressed in terms of the intensity of saturation $I_{\text{sat}} = \frac{k_f + k_e}{\sigma_s}$, this variable just consider the the fluorescent properties of the molecules. In this way we reach the expression:

$$\eta = \left[1 + \frac{\langle I_s \rangle}{I_{\text{sat}}} \right]^{-1}. \quad (14)$$

The above expression is well know in the super-resolution imaging community and have been used in theoretical and experimental contexts to assess the performance of STED microscopy.

A.2. White noise case, $\lambda \rightarrow \infty$

Using Eq. (12) we can obtain that the average population of the steady-state is given by:

$$\langle N_1(+\infty) \rangle = \frac{k_e}{K} \cdot \left[1 - \frac{\Delta}{2K^2} \right]^{-1} \quad (15)$$

Although this expression was obtained using, as a premise, the Gaussian character of the coloured noise, it can be shown that in the limit of white noise, such a result holds even if the noise have a non-Gaussian local distribution. We can now proceed with the calculation of the depletion in this scenario, which yields

$$\eta = \left[1 + \frac{\langle k_s \rangle - \frac{1}{2} \frac{\Delta}{k_f + \langle k_s \rangle + k_e}}{k_f + k_e} \right]^{-1}. \quad (16)$$

This expression shows some limitations of our mathematical model. We can notice that for $\langle k_s \rangle < \frac{1}{2} \frac{\Delta}{k_f + \langle k_s \rangle + k_e}$, the calculated depletion would be greater than one. This is a non-physical result produced by the fact that our mathematical model for $k_s(t)$ does not rule out the possibility of negative values for this quantity at large enough noise amplitudes once we have fixed $\langle k_s \rangle$. In this nonphysical scenario sufficiently high noise fluctuations in $k_s(t)$ can produce the enhancement of the values of $\langle N_1(+\infty) \rangle$ when compared to its corresponding value in the absence of the STED laser.

Rewriting the depletion in terms of $\langle I_s \rangle / I_{\text{sat}}$ we get our working expression for the depletion in the white noise limit:

$$\eta = \left[1 + \frac{\langle I_s \rangle}{I_{\text{sat}}} - \frac{\alpha^2}{2} \frac{\left(\frac{\langle I_s \rangle}{I_{\text{sat}}} \right)^2}{1 + \frac{\langle I_s \rangle}{I_{\text{sat}}}} \right]^{-1}, \quad (17)$$

where $\alpha = \frac{\sqrt{\Delta}}{\langle k_s \rangle}$, is a quantity that characterizes the laser noise distribution giving us the relative standard deviation (rsd) of the STED laser. This equation links the rsd of the laser to the final depletion efficiency obtained at a given STED power. This model is expected to better describe the CW-STED depletion curve as it depends not only on the sample properties but also on the noise properties of the depletion laser. In the absence of laser noise ($\Delta = 0$), Eq. 17 reduces to the well-known noise-free depletion expression for CW-STED microscopy.

In Fig. 2, we study the behaviour of the depletion varying the strength of the noise (Δ) and the inverse of the characteristic correlation time (λ) in different scenarios. The depletion as a function of the saturation factor $\frac{\langle I_s \rangle}{I_{\text{sat}}}$, represented as ζ in what follows was studied numerically. The fig. 2 (a) shows the behaviour of the depletion (η) in three different scenarios: ideal case ($\alpha = 0$), coloured noise ($\alpha \neq 0$ and $0 < \lambda < +\infty$) and white noise ($\lambda \rightarrow \infty$). As expected, the optimal depletion curve corresponds to the ideal case, in which the laser noise is absent [9]. On the other hand, when the noise is present our theory confirms that the higher the intensity noise the lower the depletion efficiency for a given average intensity. For instance, a noise intensity of 0.6 rsd will need a saturation factor of roughly 20 to reach the same fluorescence quenching obtained with a saturation factor of 14, in the case of a noise intensity of 0.2 rsd (figure

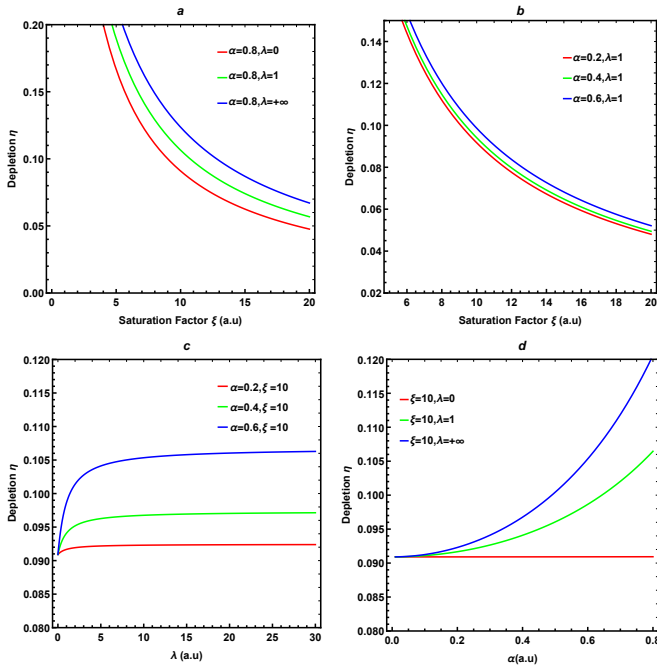


Fig. 2. Theoretical calculation of the laser intensity noise effect on the performance of the CW-STED microscopy. (a) Depletion curves corresponding to coloured noises with different correlation times, the corresponding values of the characteristic correlation time are indicated in the inset of the figure. (b) Depletion curves for different noise strengths (0.2 rsd, 0.4 rsd and 0.6 rsd) fixing the correlation time of the coloured noise. (c) and (d) Behavior of the depletion efficiency for a given saturation factor ($\zeta=10$) varying the noise strength and the correlation time, respectively.

2(a)). The presence of fluctuations deteriorates the depletion i.e. the higher the laser stability, the higher the depletion efficiency, see Fig. 2 (b). In the low-intensity noise regime ($\text{rsd} < 0.2$), depletion efficiency is not significantly affected. However, when the strength of the noise is high enough ($\text{rsd} > 0.6$), the decrease in efficiency can no longer be neglected. An increase of the variance of the noise results in a suboptimal depletion efficiency and an increase of the intensity of the STED beam is needed to recover the depletion efficiency of low noise scenario. In Fig. 2 (c) and (d), we observe that at a given saturation factor the depletion is strongly affected by an increase of α and the inverse of the correlation time of the noise (λ), in a way that systems with a higher α (λ) are more affected by an increase of λ (α).

A.3. Simulation

The analytical predictions obtained until here were verified through the numerical solution of Eq. 3 using well-established routines developed in the Mathematica 11 software [17]. The stationary population average and consequently the numerical depletion was estimated considering a large number of noise realizations $\beta(t)$. The latter was taken so that the difference between the analytical prediction and the corresponding numerical average is always less than 5%. Fig. 3 b-d shows the comparison between the analytical and numerical results for the general case of colored noise at different noise strengths. As can be seen, a good agreement is obtained, which validates the analytical predictions. In addition, we perform simulations for the limit

case of white noise (results not shown), obtaining the same level of agreement.

A.4. Comparison of theory with experimental results

Having validated our analytical model, we fit experimental depletion curves, previously published [9], to the analytical expressions. For simplicity, we used only those obtained for the white noise limit, Eq. 17. Two CW depletion lasers with the same average intensity but with different intensity noise profiles are investigated, see Fig. 4. The Low Noise Laser (LNL) has a normal distribution (0.01 rsd), while the High Noise Laser (HNL) has an unknown distribution (0.34 rsd). The measurement time was long enough to assume that the equilibrium was reached. From the fit of the experimental curves, we extracted the saturation intensity (I_{sat}) of the fluorophore and the noise (rsd) of the STED laser. No significant changes were found for low-noise scenarios when fitting the experimental curve with our model and the noise-free depletion curve, Eq. 14. These two models are statistically consistent. Previous work [9] empirically introduced a constant offset α in the noise-free depletion curve model, i.e., $\eta_{\text{noise}}(I_s) = (1 - \alpha)\eta(I_s) + \alpha$ to explain reduction of depletion efficiency for high-noise scenarios. It should be noted that the model obtained here offers an analytical expression for such scenarios. The experimental depletion curves are well described by the model with fitted parameters $I_{\text{sat}} = 5.09 \text{ MWcm}^{-2}$ and $\alpha = 1.45$ for the HNL and $I_{\text{sat}} = 5.96 \text{ MWcm}^{-2}$ and $\alpha = 0.45$ for the LNL. On the other hand, at high intensities, there is a small deviation between our theoretical curves and those obtained experimentally. A possible explanation for this effect is related to the incomplete decay of the depletion curves due to the signal background caused by the excitation from the STED beam (anti-Stokes emission) [6]. Overall, the model works well for both scenarios, high and low noise, with an adjusted R-squared value of 0.98, giving a good agreement with the previously published experimental data [9]. Finally, since the colored noise model has the Gaussian white noise model as a limiting case, it is expected that the fits using the colored noise will also work. At least we will always have the trivial solution in which the correlation time resulting from the fit is a small quantity. On the other hand, given that the experimental data have a non-negligible noise level, it will be impossible to establish which of the two theoretical models is more appropriate to describe the experiments. The chi-square test in both cases yields similar values.

A.5. Discussion and Conclusions

This letter theoretically demonstrated the importance of using stable lasers to reduce the sample illumination on CW-STED implementations. The use of a noise-eater is strongly recommended to stabilize the amplitude of a high-noise depletion laser. On the other hand, laser power stability lower the intensity to reach a certain resolution [18–20], thus they reduce potential photodamage effects and re-excitation caused by the depletion laser [6].

As we have shown, intensity fluctuations play a negative role in the performance of CW-STED microscopy. However, controlled variations of the STED intensity induces spatially encoded variations of the fluorescence emission that can, in principle, be decoded to further improve the effective spatial resolution of the STED image [21, 22]. As a result, if these fluctuations are adequately detected, one can exploit the ‘natural’ changes of STED intensity during the image acquisition and separate photons based on the depletion dynamics in the phasor plot.

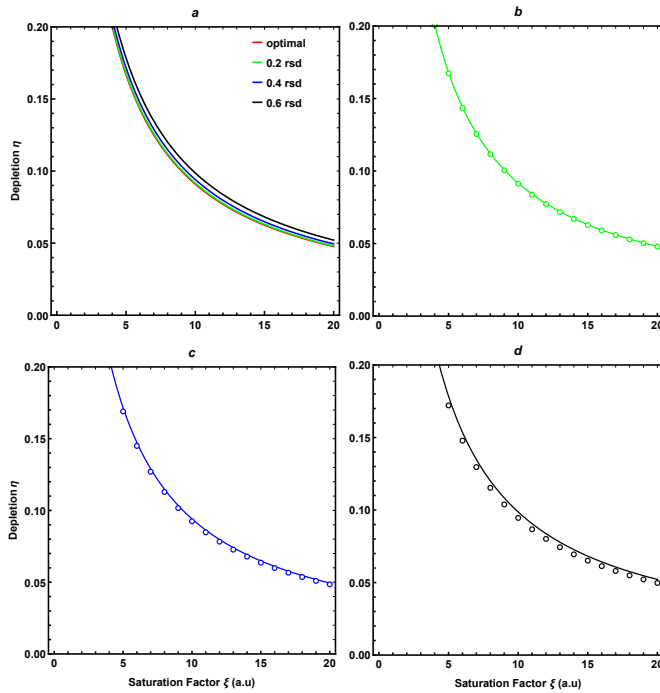


Fig. 3. Influence of colored noise intensity on depletion efficiency of CW-STED microscopy. (a) Theoretical depletion curves at different noise strengths (0.2 rsd, 0.4 rsd, and 0.6 rsd). (b-d) Comparison between analytical (full line) and computational (empty circles) simulation results for depletion as a function of saturation factor. The relative difference between theoretical and computational results for the different noise strengths 0.2 rsd, 0.4 rsd and 0.6 rsd was less than 2%, 3% and 5%, respectively.

In conclusion, this work introduces an analytical formulation capable of accurately describe the impact of intensity fluctuations and intensity correlation time on the performance (depletion efficiency) of a CW-STED microscope. The effects of noise intensity on image resolution can be understood by considering the linear proportionality relationship of this quantity with the depletion efficiency [11]. Comparison with numerical simulations and previously published experimental data validated the analytical results. The analytical approach followed here can easily be extended to other imaging modalities, such as ground-state depletion and RESOLFT microscopy [23, 24]. In future works, we will investigate the effects of time jitter and donut variability (shape and polarization) on efficiency of the STED microscope [25].

Acknowledgment. The Berthiaume Family Foundation supported this study. In addition, the authors thank Giuseppe Vicidomini (Istituto Italiano di Tecnologia) and Luca Lanzano (University of Catania) for helpful comments on the article. We also thank Nate Jowett for proofreading the manuscript. Finally, A.M.C. acknowledges financial support from Fundação de Amparo à Pesquisa de Santa Catarina FAPESC.

Disclosures. The authors declare no conflicts of interest.

Data Availability. Data underlying the results presented in this paper are not publicly available at this time but may be obtained from the authors upon reasonable request.

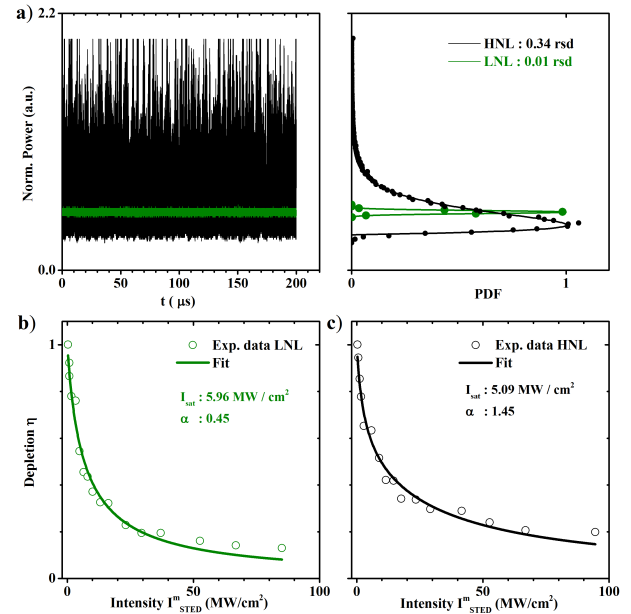


Fig. 4. Effect of laser fluctuations in CW-STED microscopy. (a) Characterization of the intensity of the two lasers based on representative time traces of 200 μs length (sampling 1 ns). The right panel displays the normalized Probability Density Functions of the two lasers. (b-c) Depletion curves measured with Alexa 488-labeled antibody (empty dots) and their corresponding fit (lines) according to the white-noise model proposed in Eq. 17.

REFERENCES

- S. W. Hell and J. Wichmann, "Breaking the diffraction resolution limit by stimulated emission: stimulated-emission-depletion fluorescence microscopy," *Opt. Lett.* **19**, 780 (1994).
- G. Vicidomini, P. Bianchini, and A. Diaspro, "STED super-resolved microscopy," *Nat. Methods* **15**, 173–182 (2018).
- G. Vicidomini, I. C. Hernández, M. d'Amora, F. C. Zanacchi, P. Bianchini, and A. Diaspro, "Gated cw-sted microscopy: a versatile tool for biological nanometer scale investigation," *Methods* **66**, 124–130 (2014).
- K. I. Willig, B. Harke, R. Medda, and S. W. Hell, "STED microscopy with continuous wave beams," *Nat. Methods* **4**, 915–918 (2007).
- C. Eggeling, A. Honigsmann, and M. Schulze, "gSTED Microscopy with an OPSP: Cutting Edge Super-Resolution," *Optik & Photonik* **7**, 44–46 (2012).
- I. Coto Hernández, C. Peres, F. Cella Zanacchi, M. d'Amora, S. Christodoulou, P. Bianchini, A. Diaspro, and G. Vicidomini, "A new filtering technique for removing anti-stokes emission background in gated cw-sted microscopy," *J. biophotonics* **7**, 376–380 (2014).
- V. Mueller, C. Eggeling, H. Karlsson, and D. Von Gegerfelt, "Cw dpss lasers make sted microscopy more practical," *Biophotonics* **19**, 30–32 (2012).
- R. Paschotta, "Noise in laser technology: Part 1: Intensity and phase noise," *Optik & photonik* **4**, 48–50 (2009).
- I. Coto Hernández, M. d'Amora, A. Diaspro, and G. Vicidomini, "Influence of laser intensity noise on gated cw-sted microscopy," *Laser Phys. Lett.* **11**, 095603 (2014).
- A. Bodén, X. C. Moreno, B. K. Cooper, A. G. York, and I. Testa, "Predicting resolution and image quality in resolft and other point scanning microscopes," *Biomed. Opt. Express* **11**, 2313–2327 (2020).
- G. Vicidomini, I. C. Hernandez, A. Diaspro, S. Galiani, and C. Eggeling, "The importance of photon arrival times in sted microscopy," in *Advanced photon counting*, (Springer, 2014), pp. 283–301.

12. C. Van den Broeck, J. Parrondo, R. Toral, and R. Kawai, "Nonequilibrium phase transitions induced by multiplicative noise," *Phys. Rev. E* **55**, 4084 (1997).
13. J. García-Ojalvo and J. Sancho, *Noise in spatially extended systems* (Springer Science & Business Media, 2012).
14. C. W. Gardiner *et al.*, *Handbook of stochastic methods*, vol. 3 (Springer Berlin, 1985).
15. L. Elsgolts *et al.*, *Differential equations and the calculus of variations* (Mir Publishers, 1970).
16. M. Kardar, *Statistical physics of fields* (Cambridge University Press, 2007).
17. W. R. Inc., "Mathematica, Version 11.0.0," Champaign, IL, 2019.
18. M. Leutenegger, C. Eggeling, and S. W. Hell, "Analytical description of STED microscopy performance," *Opt. Express* **18**, 26417 (2010).
19. J. R. Moffitt, C. Osseforth, and J. Michaelis, "Time-gating improves the spatial resolution of STED microscopy," *Opt. Express* **19**, 4242 (2011).
20. G. Vicidomini, A. Schönle, H. Ta, K. Y. Han, G. Moneron, C. Eggeling, and S. W. Hell, "STED Nanoscopy with Time-Gated Detection: Theoretical and Experimental Aspects," *PLoS ONE* **8** (2013).
21. M. J. Sarmiento, M. Oneto, S. Pelicci, L. Pesce, L. Scipioni, M. Faretta, L. Furia, G. I. Dellino, P. G. Pelicci, P. Bianchini *et al.*, "Exploiting the tunability of stimulated emission depletion microscopy for super-resolution imaging of nuclear structures," *Nat. communications* **9**, 1–11 (2018).
22. L. Lanzano, I. C. Hernández, M. Castello, E. Gratton, A. Diaspro, and G. Vicidomini, "Encoding and decoding spatio-temporal information for super-resolution microscopy," *Nat. communications* **6**, 1–9 (2015).
23. S. W. Hell and M. Kroug, "Ground-state-depletion fluorescence microscopy: A concept for breaking the diffraction resolution limit," *Appl. Phys. B* **60**, 495–497 (1995).
24. I. Testa, N. T. Urban, S. Jakobs, C. Eggeling, K. I. Willig, and S. W. Hell, "Nanoscopy of living brain slices with low light levels," *Neuron* **75**, 992–1000 (2012).
25. B. Neupane, F. Chen, W. Sun, D. T. Chiu, and G. Wang, "Tuning donut profile for spatial resolution in stimulated emission depletion microscopy," *Rev. Sci. Instruments* **84**, 043701 (2013).